Frequency and Voltage Dependence of the Dielectrophoretic Trapping of Short Lengths of DNA and dCTP in a Nanopipette

Liming Ying,* Samuel S. White,* Andreas Bruckbauer,* Lisa Meadows,† Yuri E. Korchev,‡ and David Klenerman*

*Department of Chemistry, University of Cambridge, Cambridge, CB2 1EW, United Kingdom; †Department of Genetics, University of Cambridge, Cambridge, CB2 1GA, United Kingdom; and ‡MRC Clinical Science Center, Division of Medicine, Imperial College School of Medicine, London, W12 0NN, United Kingdom

ABSTRACT The study of the properties of DNA under high electric fields is of both fundamental and practical interest. We have exploited the high electric fields produced locally in the tip of a nanopipette to probe the motion of double- and single-stranded 40-mer DNA, a 1-kb single-stranded DNA, and a single-nucleotide triphosphate (dCTP) just inside and outside the pipette tip at different frequencies and amplitudes of applied voltages. We used dual laser excitation and dual color detection to simultaneously follow two fluorophore-labeled DNA sequences with millisecond time resolution, significantly faster than studies to date. A strong trapping effect was observed during the negative half cycle for all DNA samples and also the dCTP. This effect was maximum below 1 Hz and decreased with higher frequency. We assign this trapping to strong dielectrophoresis due to the high electric field and electric field gradient in the pipette tip. Dielectrophoresis in electrodeless tapered nanostructures has potential applications for controlled mixing and manipulation of short lengths of DNA and other biomolecules, opening new possibilities in miniaturized biological analysis.

INTRODUCTION

The study of the physical properties of DNA is of both fundamental and applied interest. DNA is a highly charged polyelectrolyte with different mechanical properties in its single- and double-stranded state and hence experimental studies of DNA can test and refine polymer theory. DNA also plays a central role in modern molecular biology, so new methods to concentrate, trap, size, and separate DNA molecules have considerable analytical applications. Current interest has focused on miniaturization of methodologies down to the nanoscale and the development of gel-free techniques. Significant advances have been achieved recently in DNA separation and manipulation by using α-hemolysin nanopores (Howorka et al., 2001; Kasianowicz et al., 1996; Meller et al., 2001; Vercoutere et al., 2001), ion beam nanofabricated solid-state nanopores (Li et al., 2001), a micromachined Brownian ratchet device (Bader et al., 1999), and an engineered entropic trap array (Han and Craighead, 2000).

DNA molecules in solution have a compensating cloud of counterions that are readily polarized by an electric field. This means a dipole can be induced by application of an external electric field. This induced dipole has few consequences in the quasistatic, homogeneous electric fields that are usually applied in electrophoresis of DNA (Asbury and van den Engh, 1998). However, in a spatially nonuniform oscillating electric field, the DNA molecules may experience positive or negative dielectrophoretic forces depending on the field strength, field gradient, and frequency as well as the dielectric properties of DNA and surrounding medium (Jones, 1995). Theoretical work by Ajdari and Prost (1991) has suggested that trapping by induced-dipole forces together with free-flow electrophoresis could improve the selectivity of conventional gel-based sieving methods for DNA separation. Washizu and Kurosawa (1990) were the first to use dielectrophoretic force to manipulate kilobase DNA in a microfabricated structure. Later Asbury and van den Engh (1998) have reported DNA trapping in an oscillating electric field using stripes of thin gold film. They have also shown that trapped molecules can be moved from one edge to another by mixing static and oscillating fields. Zilberstein et al. have reported the nonlinear focusing of DNA in a wedge gel with hyperbolic geometry (Frumin et al., 2001). More recently, Austin and co-workers have demonstrated electrodeless dielectrophoretic trapping of kilobase lengths of single- and double-stranded DNA in a nanofabricated device using 1-μm diameter constrictions. In this case there are no problems with possible damage to biological molecules due to electrochemistry on metal electrodes (Chou et al., 2002).

Nanometer scale pipettes are particularly useful for material transport and scanning nanolithography (Hong et al., 2000; Lewis et al., 1999). The pipettes we used have an inner diameter of 100 nm with the voltage drop occurring within a few microns of the tip due to the taper. This means high electric fields can be generated by the application of modest voltages and therefore electrochemical effects are reduced. We have discovered that pulsatile delivery of DNA molecules can be realized in a simple way with high precision and submicrometer DNA and protein features can be written on surface under physiological conditions by using nanopipettes (Bruckbauer et al., 2002; Ying et al., 2002). In this work we have used confocal fluorescence

Submitted May 22, 2003, and accepted for publication October 8, 2003.

Address reprint requests to David Klenerman, Tel.: +44-1223-336481; Fax: +44-1223-336362; E-mail: dk10012@cam.ac.uk.

0006-3495/04/02/1018/10 $2.00

microscopy to study DNA molecules in the tip and probe dielectrophoretic effects. This offers significantly higher sensitivity and time resolution than previous studies by others using intercalator dyes and has allowed us to study significantly smaller molecules, such as 40 bases of DNA and even a single nucleotide.

The physics in the tip of the pipette is complex because the conditions are nonequilibrium. There are three contributions to the observed flow. Firstly there is electroosmotic flow, which results in plug-like flow of the solution in the pipette. The electroosmotic flow velocity is given by

$$\mathbf{u}_{\mathrm{EO}} = \mu_{\mathrm{EO}}\mathbf{E}, \tag{1}$$

where μ_{EO} is the electroosmotic mobility of the DNA and should be independent of DNA length but depends on the chemical nature of the wall material. For the silica pipettes used in this work, the direction of the electroosmotic flow (EOF) is out of the pipette on application of negative potential relative to the pipette. Secondly there is electrophoretic flow; the electrophoretic velocity is given by

$$\mathbf{u}_{\mathrm{EP}} = \mu_{\mathrm{EP}}\mathbf{E}, \tag{2}$$

where μ_{EP} is the electrophoretic mobility of the DNA. In the case of DNA there is only a weak dependence of mobility with length. A modest increase in mobility with length is observed and reaches a constant plateau at 400 DNA bases (Allison et al., 2001). This is due to the fact that the charge to mass ratio is constant for DNA of all lengths and hence gel-free separation is not possible. The electrophoretic flow will be out of the pipette upon application of a positive potential relative to the pipette. Lastly there is dielectrophoresis, (see review by Hughes (2000)). For small particles (low Reynolds numbers) the instantaneous velocity is proportional to the dielectrophoretic force (Morgan et al., 1999)

$$\mathbf{u}_{\mathrm{DEP}} = \frac{\mathbf{F}_{\mathrm{DEP}}}{f}, \tag{3}$$

where f is the frictional factor for the particle and $\mathbf{F}_{\mathrm{DEP}}$ is the dielectrophoretic force (Pohl, 1978)

$$\mathbf{F}_{\mathrm{DEP}} = 2\pi r^3 \varepsilon_{\mathrm{m}} \mathrm{Re}[f_{\mathrm{CM}}] \nabla |\mathbf{E}_{\mathrm{rms}}|^2, \tag{4}$$

where r is the radius of the particle, $\mathbf{E}_{\mathrm{rms}}$ is the local (rms) electric field, ε_{m} is the absolute permittivity of the medium, ∇ is the del (or nabla) vector operator, and $\mathrm{Re}[f_{\mathrm{CM}}]$ indicates the real part of the Clausius-Mossotti factor. Substituting for $\mathbf{F}_{\mathrm{DEP}}$ in Eq. 3 gives

$$\mathbf{u}_{\mathrm{DEP}} = \mu_{\mathrm{DEP}} \nabla |\mathbf{E}_{\mathrm{rms}}|^2, \tag{5}$$

where μ_{DEP} is the dielectrophoretic mobility. For a one-dimensional case a simple formula can be derived for the dielectrophoretic force

$$\mathbf{F}_{\mathrm{DEP}} = \alpha |E| \frac{d\mathbf{E}}{dx}, \tag{6}$$

where α is the polarizability of the DNA and $|E|$ is the scalar magnitude of the electric field (Chou et al., 2002). We work at low frequency where the polarizability of DNA is believed to be dominated by the DNA chain and particularly the counterion cloud becomes distorted on application of an electric field giving rise to a large induced dipole (Bakewell et al., 2000). The size of induced dipole forces depends on the polarizability of the DNA, which should vary with length. The dependence of the dielectrophoretic effect with DNA length opens up the possibility to separate and size the DNA without the use of gels.

In this work we have performed a detailed study of the behavior of a single nucleotide triphosphate, a single-stranded (ss) and double-stranded (ds) 40 mer of DNA and a single-stranded 1 kb of DNA in the nanopipette as function of the frequency and amplitude of the driving voltage. This has enabled us to understand qualitatively the relative contributions of the physical factors that control the motion of the DNA in the nanopipette. The results demonstrate the feasibility of trapping and controlled launching of short lengths of DNA and nucleotide triphosphates using a tapered nanostructure.

METHOD

Sample preparation

A 1 kb dsDNA polymerase chain reaction (PCR) product was amplified from *Drosophila melanogaster* genomic DNA using forward and reverse primers specific for the Hsp-68 gene region, GenBank accession number AE003746 (Forward primer: 5′-ACC CTT GTC GTT CTT GAT GG-3′; Reverse primer: 5′-GGC CTG GAC AAG AAT CTG AA-3′). The product was diluted 1:1000 and used as the template for a further PCR with only the reverse primer and the following nucleotide concentrations: 0.2 mM dATP, dGTP, dTTP, 0.18 mM dCTP, and 0.02 mM Cy5-dCTP (PA 55021, Amersham Biosciences, Amersham, UK), to generate ssDNA 1 kb in length with Cy5-dCTP incorporated throughout. The labeled product was purified by passing it through an AutoSeq G-50 column according to manufacturer's protocol (27-5340-02, Amersham Biosciences).

Cy5-labeled dCTP (CyDye) was obtained from Amersham Biosciences. The 40-base oligonucleotide, synthesized by MWG-Biotech (Ebersberg, Germany) is 5′-TAG TGT AAC TTA AGC CTA GGA TAA GAG CCA GTA ATC GGT A-3′, an unlabeled version, and a 5′-labeled with fluorophore rhodamine green (RG) version were produced (all HPLC purified). Its complementary 40-base oligonucleotide with a 5′ C6 amino modifier (Transgenomic, Glasgow, UK) was desalted (NAP 5 column, Amersham) and labeled with an Alexa Fluor 647 Oligonucleotide Amine Labeling Kit (Molecular Probes, Leiden, The Netherlands) following the manufacturer's instructions. The labeled oligonucleotide was separated from the excess dye using a Sephadex 25 (Amersham) column followed by ethanol precipitation, and then from unlabeled DNA by gel electrophoresis. The bands containing labeled oligonucleotide were identified by visual inspection and ultraviolet (UV) shadowing. They were excised and the DNA eluted into 10 mM Tris-HCl using the ''crush and soak'' method. The oligonucleotide was purified by extraction with phenol:chloroform:isoamyl alcohol 25:24:1, ethanol precipitation, and desalting with a NAP 5 column. Single fluorophore-labeled (Alexa-647) double-stranded DNA (dsDNA) samples were prepared by hybridizing the unlabeled 40-base oligonucleotide and its complementary Alexa-647-labeled strand.

The ss 35-base DNA sample was synthesized by Cruachem (Glasgow, UK) and was HPLC purified. The sequence of the DNA is 5′-CTA TGC

AGC CAT TGT AGT CCC GCA ACA CCT CGA GT-3′. The 3′ end was modified by rhodamine green (Molecular Probes), and the 5′ end was modified with biotin. The concentration of the dye-labeled DNA was determined by UV-visible absorption at 260 nm, and the absorption at 504 nm was used as an internal reference.

The nanopipettes were made using a laser-based pipette puller (Model P-2000, Sutter Instrument, Novato, CA), a two-line program was used to pull borosilicate glass capillaries (inner diameter, 0.58 mm; outer diameter, 1 mm) with the following parameters:

$$\text{Heat} = 350,\ \text{Fil} = 3,\ \text{Vel} = 30,\ \text{Del} = 220,\ \text{Pull} =$$

$$\text{Heat} = 330,\ \text{Fil} = 2,\ \text{Vel} = 27,\ \text{Del} = 180,\ \text{Pull} = 250.$$

Tris-HCl and EDTA buffer solution (0.2 μm filtered) was purchased from Amersham Life Sciences and NaCl (DNase, RNase, and protease-free) from Acros Organics (Fairlawn, NJ). The DNA solution (10–100 nM) of two oligonucleotides was backfilled to the bent nanopipette by a microfiller (Microfil 34, World Precision Instruments, Sarasota, FL). A scanning electron micrograph is shown in Fig. 1. A coverglass bottomed dish (Willco Wells GWST-1000) containing 2–3 ml solution was used as the bath. The pipette tip was placed 5–10 μm above the dish surface. Two Ag/AgCl electrodes, one in the bath and the other inside the pipette, served as the working and reference electrodes, respectively. The ion current flowing through the pipette was the same in the presence and absence of DNA because the ion current is dominated by the flow of sodium and chloride ions. In addition no ion current reduction, due to partial blocking, could be detected with DNA in the pipette. Identical buffers (10 mM Tris-HCl, 1mM EDTA, and 100 mM NaCl) were used both in the pipette and in the bath. EDTA was used to remove multivalent cations in the solution.

Experimental setup

Our two-color confocal microscope has been described previously (Li et al., 2003). Two overlapping laser beams (488 nm, Argon ion, model 35LAP321-230 and 633 nm, model 25LHP151 HeNe laser, Melles Griot, Carlsbad, CA) at ~0.25 mW and 0.15 mW, respectively, were directed through a dichroic (FITC/CY5, AHF Analysentechnik AG, Tübingen, Germany) mirror and oil immersion objective (Apochromat 60×, n.a. 1.40, Nikon, Melville, NY) to be focused 5 μm into the sample solution (Fig. 2). The red beam was adjusted to be parallel and the size was expanded to just fill the back aperture of the objective. The blue beam was also expanded by a telescope and tuned to be slightly convergent to achieve better overlap in the z-direction of the focal volume. Fluorescence was collected by the same objective and imaged onto a 50-μm pinhole (Newport, Irvine, CA) to reject out of focus fluorescence and other background. Green and red fluorescence were then separated using a second dichroic mirror (585DRLP, Omega Optical Filters, Brattleboro, VT). Green fluorescence was filtered by long-pass and band-pass filters (510ALP and 535AF45, Omega Optical Filters) before being focused onto an avalanche photodiode, APD (SPCM AQR-141, EG&G, Quebec, Canada). Red fluorescence was also filtered by long-pass and band-pass filters (565ALP and 695AF55, Omega Optical Filters) before focusing onto a second APD (SPCM AQR-141, EG&G). Outputs from the APDs were coupled to two PC-implemented multichannel scalar cards (MCS-Plus, Ortec, Canada), the synchronous start output of one MCS card being used to trigger the second. A CCD camera was used to determine and adjust the position of two beams in the x-y plane. The right position of two beams in z-direction was achieved by getting maximum cross-correlation amplitude when adjusting the telescope position. Maximum overlap between the two-laser focal volumes was found to be ~30%. The potential waveforms applied to the electrodes were created using a function generator (Model DS345, Stanford Research Systems, Sunnyvale, CA). This function generator was also used to provide a trigger for the MCS cards.

In these experiments we measure the amount of fluorescence from the fluorophore-labeled DNA or dCTP. This is proportional to the average number of molecules in the probe volume during the bin time of 1 ms. The probe volume with the laser focused at the tip of the pipette is estimated to be smaller than that outside the pipette due to constraints of the wall of the pipette. Assuming a pipette inner diameter of 100 nm and a beam waist of 260 nm we estimate the volume is 8.2×10^{-4} fl, more than two orders of magnitude smaller than the volume outside measured previously as 0.34 fl.

RESULTS

Electric field in the pipette tip

When we apply a voltage between the electrodes in the bath and the electrode in the pipette, the potential drop occurs almost entirely in the region of the pipette tip, due to the conical geometry of the pipette and its narrow aperture. Given the approximations that there is no effect of surface charge of the glass wall on the applied field and that the ion current is constant throughout the pipette, we have for the region inside the pipette

$$dV(x) = -Id\rho(x) = -\frac{I}{\pi\xi(R_0 + x\tan\theta)^2}dx, \qquad (7)$$

where ρ is the pipette resistance, x is the distance from tip, ξ is the conductivity of the buffer solution, R_0 is the radius of the tip opening, θ is the half-cone angle of the inner wall of the pipette, and V is the applied potential. When the tip radius is much smaller than the taper length of the pipette, integrating Eq. 7 we obtain

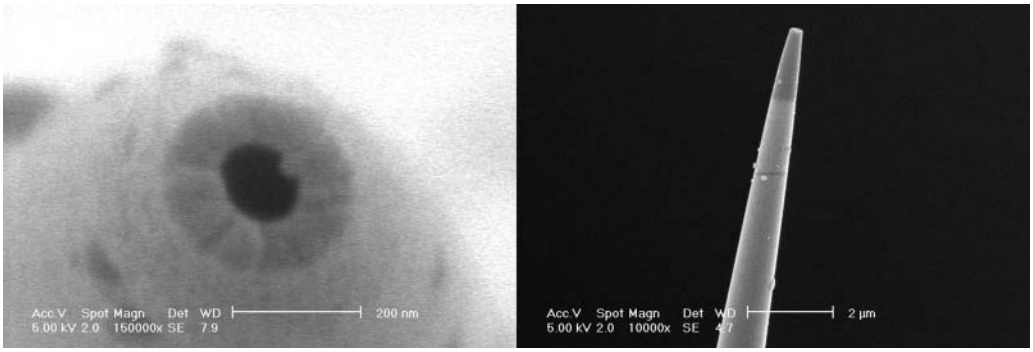

FIGURE 1 Scanning electromicrographs of the nanopipette tip coated with 5 nm of gold. The scale bar is 200 nm (*left*) and 2 μm (*right*), respectively.

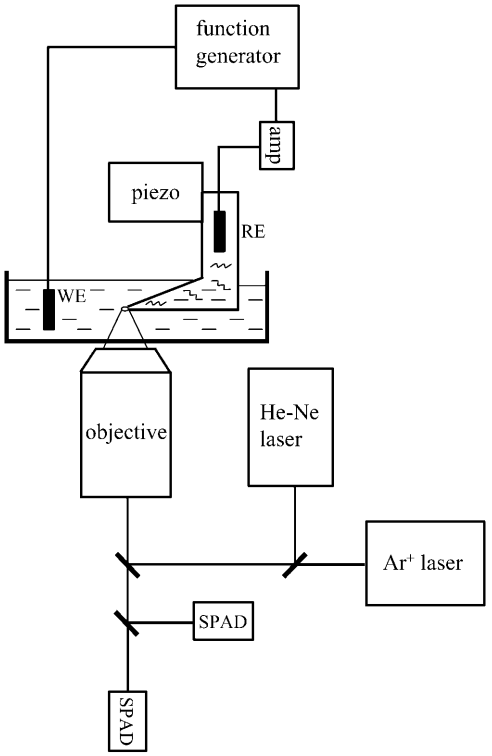

FIGURE 2 Schematic of the experimental setup. The nanopipette can be finely adjusted by an *XYZ* piezo stage, allowing the laser to be focused both inside and outside the tip opening. DNA molecules labeled with rhodamine green and Cy5 or Alexa-647 were excited by an Argon ion laser at 488 nm and a HeNe laser at 633 nm. SPAD: single photon counting avalanche photodiode.

$$\rho = \frac{1}{\pi \xi R_0 \tan\theta}, \tag{8}$$

and

$$V(x) = \frac{V_0 R_0}{R_0 + x\tan\theta}. \tag{9}$$

The electric field distribution inside the pipette along the pipette axis is then simply

$$E(x) = -\frac{dV(x)}{dx} = \frac{V_0 R_0 \tan\theta}{(R_0 + x\tan\theta)^2}. \tag{10}$$

Close to the pipette opening and in the surrounding electrolyte outside the pipette we used a simple finite element approach to calculate the electric field. The region from 1 μm inside the pipette to 0.5 μm outside the pipette was defined as an axiosymmetric geometry as shown in Fig. 3 *A* (*inset*). A grid was defined to create polygonal blocks and the Poisson equation solved in each block using the program QuickField (student's edition, Tera Analysis, Svendborg, Denmark). To define the boundary conditions, the potential of the edge 1 μm inside the pipette was calculated from Eq. 9 and the potential of the edge 0.5 μm outside the pipette was set to 1.0 V. The combined results for the electric field from the finite element analysis (for $x < 0.2$ μm) and from Eq. 10 (from $x > 0.2$ μm) are shown in Fig. 3 *A*.

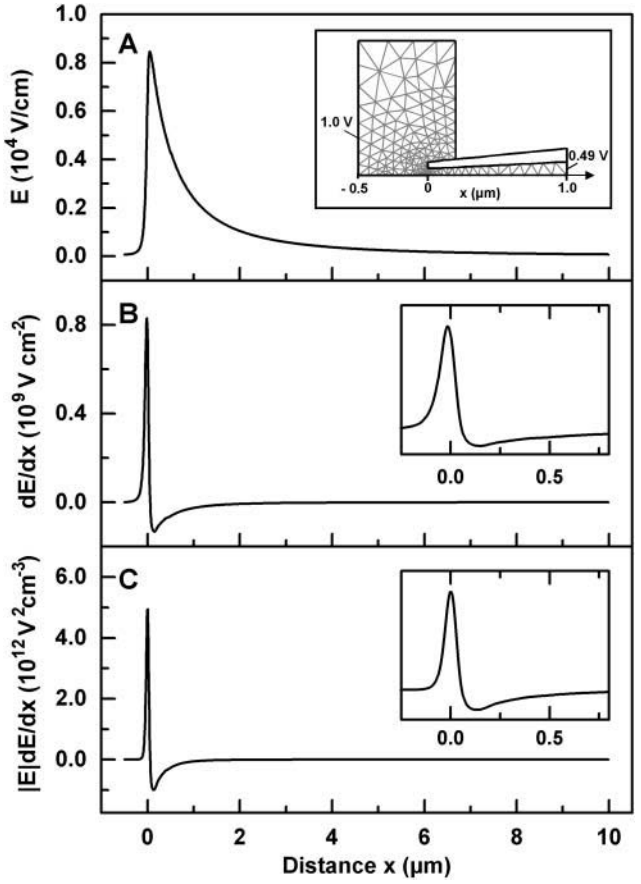

FIGURE 3 Plot of the electric field (*A*), electric field gradient (*B*), and their product (*C*) for a pipette with inner diameter of 100 nm, 6° cone angle, and 1-V applied voltage. The inset (*A*) shows the axial symmetric geometry (identical scaling in x and r) used to model the region close to the tip; the polygons depict the finite element mesh used for this analysis. The region inside the pipette ($x > 200$ nm) was calculated with Eq. 10. Insets in *B* and *C* show details close to the pipette opening.

It is clear from the above analysis that the applied electric field is highly nonuniform and will be highest inside the pipette at very short distances from the tip opening (Fig. 3 *A*). It reaches a maximum of 8000 V cm^{-1} at the pipette opening and then sharply decreases to zero outside the tip. The electric field gradient is also located very close to the tip and changes sign at the pipette opening (Fig. 3 *B*). The product of the electric field and electric field gradient shows the same characteristics with a minimum located 100 nm inside the tip and a sharp maximum at the pipette opening (Fig. 3 *C*). As we mentioned earlier, the dielectrophoretic force depends on this product. There are two types of dielectrophoretic force; positive dielectrophoresis (observed in this experiment) where particles are attracted to regions of high electric field gradients and negative dielectrophoresis where particles are repelled from regions of high electric field gradients. In these experiments the force on the DNA inside the pipette, close to

the tip, will be toward the tip. Just outside the pipette the force is back toward the tip. Therefore molecules can be trapped at the tip provided that they are not moving too fast when they enter the tip region.

Forty-mer ssDNA, 40-bp dsDNA, and dCTP at 0.5 Hz

For these experiments the voltage applied to the pipette was a sine wave at 0.5 Hz. The ss- and dsDNA behavior were studied simultaneously, by the use of two-color excitation and two-color detection, allowing both molecules to be followed in the same nanopipette. Fig. 4 shows representative data for the ss- and dsDNA in the tip and just outside the tip. These cycles were highly reproducible for this pipette. The observed behavior for the positive and negative half of the cycle is remarkably different, however both ss- and dsDNA show very similar behavior. For the positive half of the cycle the EOF flow is into the pipette and the electrophoretic flow is out of the pipette. The dielectrophoretic-induced flow is directed from inside the pipette toward the tip. Maximum DNA concentration for the positive half cycle is observed at the tip around the peak of the positive voltage cycle and the DNA also exits the pipette because the DNA is also observed outside the pipette at the same time and with similar magnitude. This indicates that the DNA is flowing out of the pipette during the positive half cycle with no trapping.

In the negative half cycle the EOF is into the pipette tip, and the electrophoretic flow is, away from the tip deeper into the pipette. The dielectrophoretic induced flow is still from inside the pipette toward the tip. In this case a large increase in DNA concentration is observed in the tip at or just after the minimum in the negative half cycle. However this DNA is trapped because no DNA is observed to flow out of the pipette. The DNA only exits the pipette when the potential gets close to zero. The DNA is released as a short pulse at this time, but only in the cases where the amplitude of the applied sine wave potential is above 2 V. When the amplitude is below 2 V the potential gradient is not large enough to enhance the concentration at the tip significantly. The same behavior is observed over a range of voltages and for both ss- and dsDNA.

Fig. 4, *E* and *F*, shows the dependence of the total integrated fluorescence signal with voltage. In the positive half cycle both the DNA in the tip and outside increase with voltage. There is also some evidence of reaching plateau above 2 V for ss- and dsDNA coming out of the pipette. Above 4 V the amount of DNA in the tip increases again but this is not mirrored by an increase of the DNA outside the pipette indicating that trapping may be commencing.

In the negative half cycle the DNA in the tip increases with voltage fairly linearly up to 4 V. Beyond this there is a decrease, which may be due to the position of the trap moving deeper into the pipette. The DNA launched from the pipette is significantly less than that trapped, presumably due to some of the DNA returning back into the pipette when the voltage reaches zero. The amount launched from the pipette initially increases with voltage, until it reaches a plateau at ~2 V, and does not show a dip at 5 V supporting the idea that the position of the trap may have moved at higher voltage.

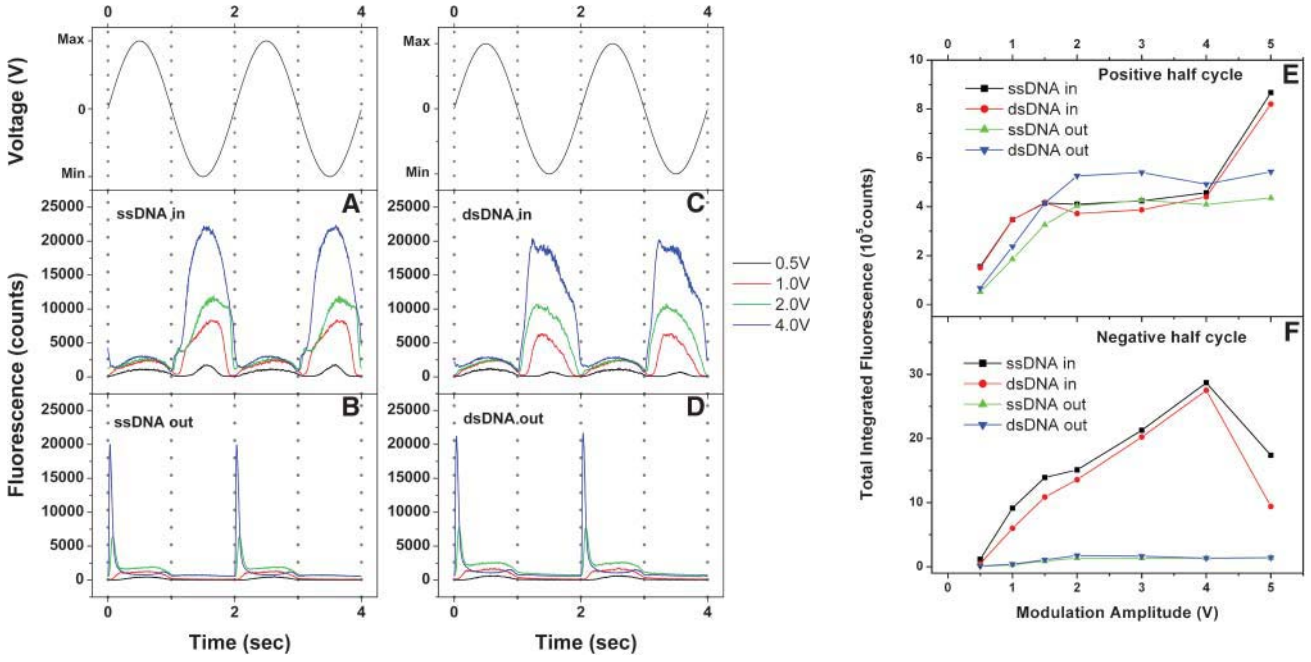

FIGURE 4 Fluorescence traces of 40-base RG-labeled ssDNA and 40-bp Alexa-647-labeled dsDNA at 0.5-Hz voltage modulation with different amplitudes. Data was collected inside the pipette (*A* and *C*) and outside the pipette (*B* and *D*). The total fluorescence intensity integrated from positive and negative half cycle of the modulation as a function of modulation amplitude is shown in *E* and *F*.

The use of simultaneous two-color detection is essential for these experiments. We have observed large variations, up to a factor of 10, for the fluorescence intensity of different pipettes even though they have similar resistance. This suggests that the electrical field and field gradient in pipette tip are much more sensitive to the pipette geometry than the pipette resistance. It also means that quantitative analysis of the data is not possible. However all the pipettes studied gave the same qualitative behavior.

We also performed experiments with dCTP in the pipette. Representative data is shown in Fig. 5, *A* and *B*, applying a 0.5-Hz sine wave. Surprisingly the dCTP shows similar behavior to 40 bases of DNA. There is clear evidence for trapping of the dCTP during the negative half cycle, because the dCTP fluorescence increases in the tip but there is a much smaller increase in fluorescence out of the pipette. A pulse of dCTP is observed outside the pipette when the voltage reaches zero due to a release of the trapped DNA. During the positive half cycle there is flow from the pipette to the bath. The voltage dependence is shown in Fig. 5, *C* and *D*; in the positive half cycle the amount of dCTP flowing out of the pipette behaves in a similar way to DNA and increases with voltage until it plateaus out around 3 V. In contrast to DNA, the amount in the pipette decreases with voltage from 1 V onwards, which is possibly due to local dCTP depletion in the tip. This indicates that virtually no trapping occurs in the tip during the positive half cycle and almost all of the dCTP flows out. Very little dCTP flows from the pipette during the negative half cycle suggesting trapping.

Low frequency and DC behavior

We studied the behavior of the 40-mer DNA on application of triangle wave at frequency of 0.01 Hz (Fig. 6). The behavior is similar to that observed at 0.5 Hz with trapping occurring in the negative half cycle. However at this low frequency we observe depletion of the DNA inside the pipette close to the maximum in the negative half cycle. This result supports the idea that the trap moves deeper into the pipette at higher voltage and then moves back as the voltage is lowered. This would give rise to the two approximately equal peaks observed. Both ss- and dsDNA showed similar behavior.

We also studied the amount of DNA in the tip as a function of time under the application of DC positive voltage (0.5 V) for the ss 35-base DNA as shown in Fig. 7. We found a linear increase with the fluorescence with time by a factor of 20 during 110 min. This is also an evidence for partial trapping of the DNA in the pipette tip leading to a concentration increase, but this time on application of a positive voltage.

Frequency dependence

Fig. 8, *A–D*, shows the dependence of the peak fluorescence intensity inside the tip of the pipette with frequency for both

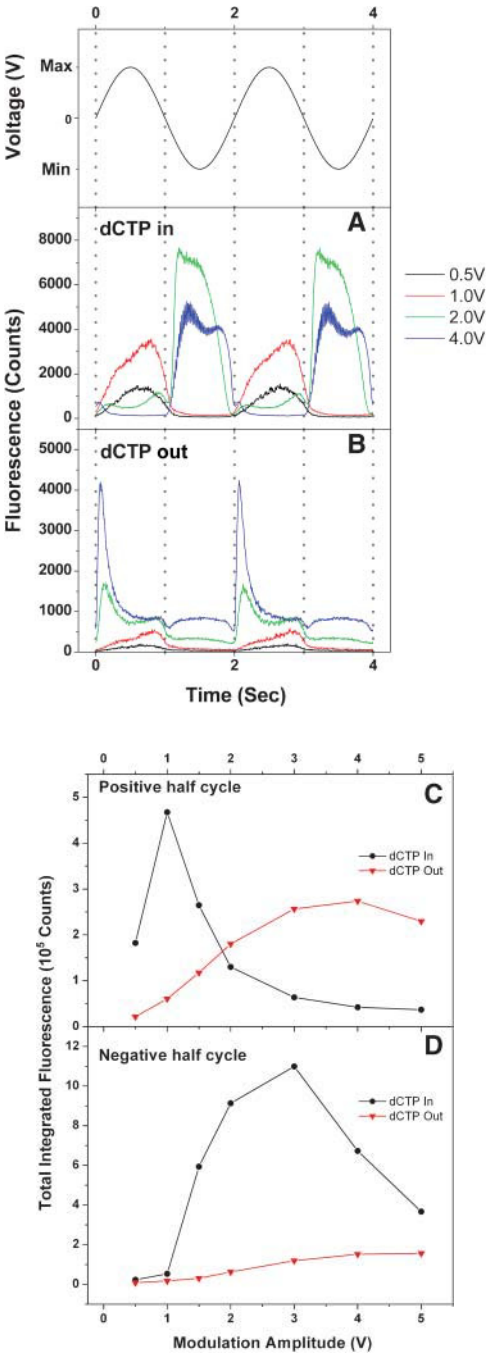

FIGURE 5 Fluorescence traces of Cy5-labeled dCTP at 0.5-Hz voltage modulation. Data was collected inside the pipette (*A*) and outside the pipette (*B*). The total fluorescence intensity integrated from positive and negative half cycle of the modulation as a function of modulation amplitude is shown in *C* and *D*.

40-base and 1-kb ssDNA. This data was taken simultaneously using the two-color method. It is clear that as the frequency increases the magnitude of the signal for the 40 mer decreases. For the 1-kb DNA it passes through a maximum at 0.4 Hz and then decreases. We analyzed both the low frequency behavior from 0.1 Hz to 1.4 Hz where the

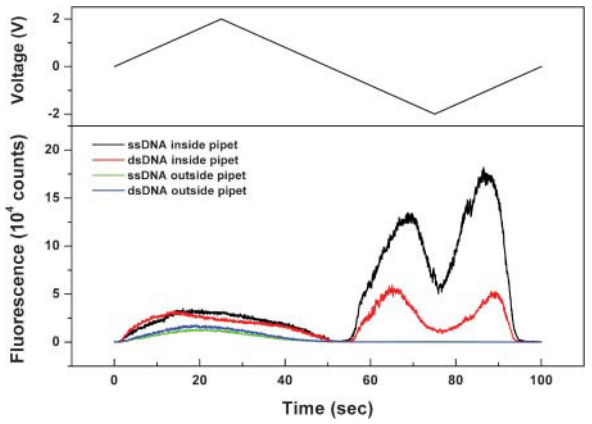

FIGURE 6 Fluorescence traces of 40-base RG-labeled ssDNA and 40-base Alexa-647-labeled dsDNA during a voltage scan (±2 V) with a 0.01-Hz scan rate. The data was collected inside and outside the pipette at 50-ms time resolution.

fluorescence from positive and negative half cycles can be resolved (Fig. 8 *E*) and also the high frequency decay of signal from 10 Hz to 1000 Hz where an averaged fluorescence from positive and negative half cycles is observed (Fig. 8 *F*). The intermediate region has not been analyzed as the integration time (100 ms) was not short enough to completely resolve the positive and negative half cycles or long enough to average them.

The effective maximum trapping potential was calculated by

$$U = -kT \ln \frac{I_{\max}}{I_{\min}}, \tag{11}$$

where $I_{\max}$ is the peak intensity and $I_{\min}$ is the minimum intensity corrected for background of one sine wave cycle. $I_{\min}$ is close to but not exactly zero. The result of this analysis is shown in Fig. 8 *E*. For both the 40-mer and 1-kb DNA a large effective potential is calculated of ~8 kT. The 1-kb DNA shows a clear minimum at 0.4 Hz whereas the 40-mer has no minimum in this frequency range.

We also analyzed the decay in signal at high frequencies (Fig. 8 *F*). Here the measured intensity is averaged because

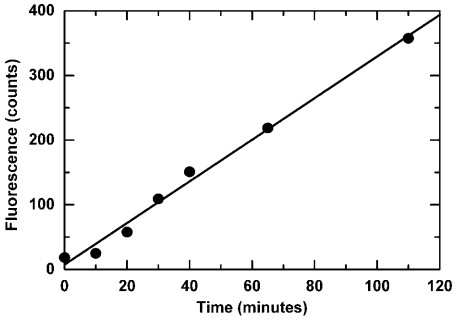

FIGURE 7 Time dependence of the fluorescence intensity at the pipette tip when a positive DC voltage of 500 mV is applied (100 nM 35-base ssDNA labeled with rhodamine green).

the bin time is longer than one cycle. The classical dielectric relaxation equation derived by Debye is often used to model single dielectric relaxation events as a function of frequency,

$$\varepsilon' = \varepsilon_u + \frac{\varepsilon_r - \varepsilon_u}{1 + \omega^2 \tau^2}, \tag{12}$$

where ε_r and ε_u represent the permittivity at very low and very high frequency, respectively, ε' is the real part of the complex permittivity in the form of $\varepsilon^* = \varepsilon' - i\varepsilon''$, and ω is the circular frequency. The ss- and dsDNA behavior was studied simultaneously. If the trapping is governed by a single relaxation process and assuming that trapping efficiency is proportional to the strength of the induced dipole, we can fit the observed fluorescence intensity inside the tip as a function of frequency to the following dispersion equation (Asbury et al., 2002)

$$I = \frac{A}{1 + 4\pi^2 f^2 \tau^2} + B, \tag{13}$$

where τ is the relaxation time (Fig. 8 *F*). This analysis fitted the data well giving a value for τ of 3.7 ms. The mean relaxation time measured from different pipettes is 4.2 ± 0.8 ms and 5.9 ± 1.3 ms for 40-mer and 1-kb DNA, respectively. These values are very close to that measured Asbury et al. (2002) using other methods. It was found that the dCTP had similar frequency dependence to the 40-mer.

DISCUSSION

The discussion that follows is largely qualitative because: 1), it is extremely difficult to calculate the magnitude of the relative flows due to dielectrophoresis, electroosmotic and electrophoretic flow in the pipette tip, and 2), there was experimental variation between pipettes. However it is possible to deduce the relative magnitude of these effects and explain our experimental observations.

We have estimated the electric field in our experiment is ~8000 V cm^{-1}, this is comparable to the electric field used by Austin and co-workers (Chou et al., 2002), and much higher than the field used by Asbury and co-workers, ~250 V cm^{-1} (Asbury et al., 2002). The velocity of DNA in the tip can be estimated using the free-solution mobility of 4×10^{-4} cm^2 V^{-1} s^{-1} (Stellwagen et al., 1997). This gives a value for a field of 8000 V cm^{-1} of 3.2 cm s^{-1} or 32 μm per ms. This velocity is very fast and the dielectrophoretic force will need to act to slow the DNA down for any trapping to occur in the pipette tip.

We have observed flow to the pipette tip during both the positive and negative half cycle. If the flow was entirely due to a combination of electrophoretic and electroosmotic flow then the flow would occur only during one or the other half cycle but not both. The observation of flow to the tip during both half cycles is clear indication of an additional flow, which is believed to be due to dielectrophoresis. Because we

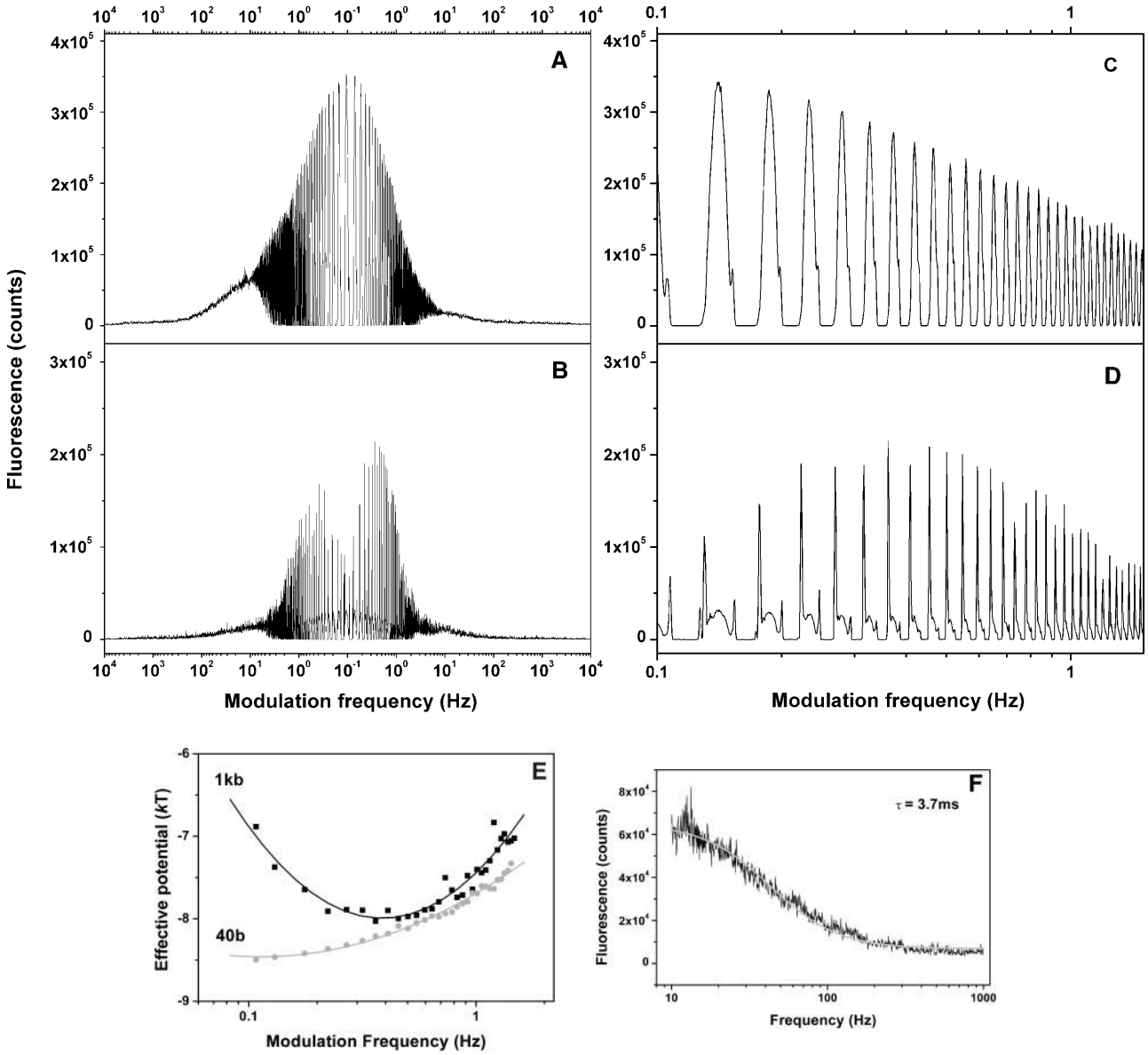

FIGURE 8 Fluorescence traces of 40-base RG-labeled ssDNA and 1000-base Cy5 labeled ssDNA. The sine wave frequency was increased logarithmically from 0.1 Hz to 10 kHz and back to 0.1 Hz in a 1000-s scan time. The data was collected inside the pipette at 100-ms time resolution and the time axis was converted into frequency. (*A* and *B*) Complete scan from 0.1 Hz to 10 kHz to 0.1 Hz for 40-base and 1000-base ssDNA, respectively; (*C* and *D*) expanded view of corresponding low-frequency region. (*E*) Effective trapping potential estimated from *C* and *D* using Eq. 11. (*F*) Fluorescence trace from 10 Hz to 100 Hz was fitted to Eq. 13 giving time constant 3.7 ms for 40-base ssDNA.

observe flow of the DNA out of the pipette during the positive half cycle this indicates that electrophoretic flow is larger than electroosmotic flow in these experiments. This may be expected because we are working at high salt and neutral pH where the electroosmotic flow is known to be low. As shown in the schematic in Fig. 9, because both the resultant flow of electrophoretic minus electroosmotic and also the dielectrophoretic flow is toward the tip in the positive half cycle, then no trapping is observed. In contrast during the negative half cycle the resultant flow of electrophoretic minus electroosmotic flow is away from the tip into the pipette and the dielectrophoretic flow is to the tip. In the region near the tip there is a net flow to the pipette tip, which is significantly smaller than that during the positive half-cycle and this results in trapping of the DNA, because it approaches the trap in the tip at a smaller velocity. Further from the tip the electrophoretic flow is larger than the dielectrophoretic flow to the tip and results in depletion of DNA in a region close to but not at the tip as shown in the schematic in Fig. 9. Once the potential is reduced to close to zero then the trapped DNA is released and a pulse of DNA of short duration is observed outside the pipette. This pulse is sharp because there is a region with no DNA close to the tip. This model suggests that the size of the electrophoretic flow

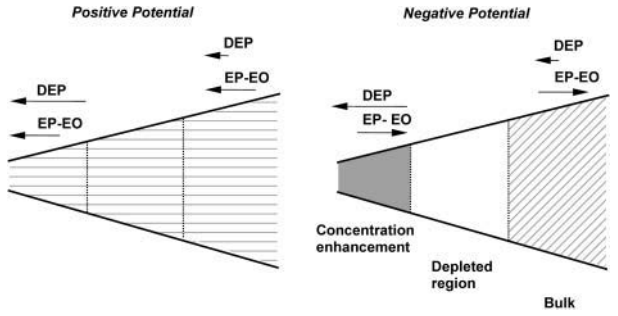

FIGURE 9 Pipette schematic showing the major forces acting on the DNA molecule when a positive or negative potential is applied.

and dielectrophoretic flow at the tip are of approximately comparable size under our experimental conditions.

The dielectrophoretic trapping is frequency dependent, a maximum trapping potential was detected for 1000 bases at 0.4 Hz and was calculated to be 7–8 kT. We also observed that the trap may not be positioned exactly at the tip but slightly deeper into the pipette particularly when larger voltages are applied. This may be due to the fact that we are working under nonequilibrium conditions, however, further work is required to address this point. There is also a heating effect due to the ion current flow but this is estimated to be <1 K due to the small current (5–40 nA) that flows.

Our observations of trapping of small DNA during a half cycle are surprising. However, our experimental setup is different from most work to date apart from Austin and co-workers (Chou et al., 2002): the pipette is an electrodeless system so there are fewer issues with surface adsorption and the pipette is a tapered nanostructure so that all the voltage drop occurs in the last few microns of the pipette tip enabling us to obtain high electric field and electric field gradients. We have also worked at low frequencies where the dielectrophoretic effect is known to be anomalously large. The observation of dCTP trapping is particularly interesting. The charge-to-mass ratio is close to the 40 bases of DNA because the labeling fluorophore Cy5 has a negative charge. The size of the effect suggests that the polarizability of DNA does not scale with length for the short DNA we have studied at low frequencies, or that for the dCTP the polarizability is dominated by the Cy5 fluorophore. This may be the more likely explanation because the dye is a conjugated molecule and significantly larger than the dCTP.

We have observed no large difference between ss- and dsDNA unlike the work by Austin and co-workers (Chou et al., 2002). It is possible that the ssDNA will be stretched in the field so would behave similarly to dsDNA, although it would be expected to have a lower polarizability. The stretching of ssDNA in the tip due to the electric field would also explain why we observed no problems with blocking when using the 1-kb-long DNA. This observation is not surprising based on work by Smith and Bendich where tethered DNA 15 μm in length was fully extended by an applied electric field of 10 V cm^{-1} (Smith and Bendich, 1990). The 40-base DNA is ~20-nm long (for ssDNA each base is ~0.5-nm long). Therefore we estimate that a field of 10^4 V cm^{-1} would be needed to fully extend it, making the simplified assumption that the same potential drop and, hence, force is required to act on the end of the DNA. Our field is of this magnitude and thus consistent with our experimental observations. This implies that this method could be applied to long lengths of DNA or possibly could be used for any charged linear polymer.

In this work we have assumed that the frequency dependence is due to dielectric relaxation. Another possibility is that as the frequency increases the DNA has less time to diffuse into the pipette tip and hence this leads to the reduction in signal. However the velocity is estimated to be 32 μm/ms so even at kHz frequency there should be sufficient time for the DNA to reach its equilibrium concentration. Furthermore the dielectric relaxation rate measured in our experiment is in good agreement with previous measurement using a different method supporting the argument that the frequency dependence is due to the dielectric relaxation.

Like the work of Austin and co-workers (Chou et al., 2002) it is not possible to model the data quantitatively. The current theory does not predict the size of the effects and in addition we have experimental variation in the voltage induced flow properties of the pipettes. The theory clearly requires further development. Our simple model suggests that an increase in taper angle would increase the size of the dielectrophoretic effect. The effect will also increase if smaller pipettes are used. It is possible to use quartz pipettes to obtain an inner diameter of down to 10 nm. The source of the observed variation also needs more investigation because the pipettes all have similar resistance and are pulled using identical pulling parameters. It should also be possible to produce tapered nanostructures with less variation in flow characteristics using focused ion beam milling and nanolithographic methods.

Our observation of trapping of small molecules suggests that dielectrophoretic trapping may be applicable to many small molecules, which has not been observed because of the methods used to study dielectrophoresis to date. The main requirement is the need for tapered nanostructure so the potential drop is localized. In this work we have created only a half trap and no trapping occurs during the positive half cycle. To make a full trap one would need a symmetric structure that reduces to a taper and then reexpands again. It should be possible to make such tapered structure in two dimensions using nanofabrication methods. Such structures may serve as valves for controlled mixing and manipulation of DNA and other molecules opening new possibilities in miniaturized biological analysis.

We thank T. Burgess for obtaining the scanning electron microscopy images at the MuitiImaging Center, University of Cambridge, Cambridge, UK. We also acknowledge valuable discussions with T. Duke.

This work was supported by the Biotechnology and Biological Sciences Research Council.

REFERENCES

Ajdari, A., and J. Prost. 1991. Free-flow electrophoresis with trapping by a transverse inhomogeneous field. *Proc. Natl. Acad. Sci. USA.* 88:4468–4471.

Allison, S., C. Y. Chen, and D. Stigter. 2001. The length dependence of translational diffusion, free solution electrophoretic mobility, and electrophoretic tether force of rigid rod-like model duplex DNA. *Biophys. J.* 81:2558–2568.

Asbury, C. L., A. H. Diercks, and G. van den Engh. 2002. Trapping of DNA by dielectrophoresis. *Electrophoresis.* 23:2658–2666.

Asbury, C. L., and G. van den Engh. 1998. Trapping of DNA in nonuniform oscillating electric fields. *Biophys. J.* 74:1024–1030.

Bader, J. S., R. W. Hammond, S. A. Henck, M. W. Deem, G. A. McDermott, J. M. Bustillo, J. W. Simpson, G. T. Mulhern, and J. M. Rothberg. 1999. DNA transport by a micromachined Brownian ratchet device. *Proc. Natl. Acad. Sci. USA.* 96:13165–13169.

Bakewell, D. J., I. Ermolina, H. Morgan, J. Milner, and Y. Feldman. 2000. Dielectric relaxation measurements of 12 kbp plasmid DNA. *Biochim. Biophys. Acta.* 1493:151–158.

Bruckbauer, A., L. M. Ying, A. M. Rothery, D. J. Zhou, A. I. Shevchuk, C. Abell, Y. E. Korchev, and D. Klenerman. 2002. Writing with DNA and protein using a nanopipet for controlled delivery. *J. Am. Chem. Soc.* 124:8810–8811.

Chou, C. F., J. O. Tegenfeldt, O. Bakajin, S. S. Chan, E. C. Cox, N. Darnton, T. Duke, and R. H. Austin. 2002. Electrodeless dielectrophoresis of single- and double-stranded DNA. *Biophys. J.* 83:2170–2179.

Frumin, L. L., S. E. Peltek, and G. V. Zilberstein. 2001. Nonlinear focusing of DNA macromolecules. *Phys. Rev. E.* 6402:021902.

Han, J., and H. G. Craighead. 2000. Separation of long DNA molecules in a microfabricated entropic trap array. *Science.* 288:1026–1029.

Hong, M. H., K. H. Kim, J. Bae, and W. Jhe. 2000. Scanning nanolithography using a material-filled nanopipette. *Appl. Phys. Lett.* 77:2604–2606.

Howorka, S., S. Cheley, and H. Bayley. 2001. Sequence-specific detection of individual DNA strands using engineered nanopores. *Nat. Biotechnol.* 19:636–639.

Hughes, M. P. 2000. AC electrokinetics: applications for nanotechnology. *Nanotechnology.* 11:124–132.

Jones, T. B. 1995. Electromechanics of Particles. Cambridge University Press, Cambridge, UK.

Kasianowicz, J. J., E. Brandin, D. Branton, and D. W. Deamer. 1996. Characterization of individual polynucleotide molecules using a membrane channel. *Proc. Natl. Acad. Sci. USA.* 93:13770–13773.

Lewis, A., Y. Kheifetz, E. Shambrodt, A. Radko, E. Khatchatryan, and C. Sukenik. 1999. Fountain pen nanochemistry: atomic force control of chrome etching. *Appl. Phys. Lett.* 75:2689–2691.

Li, H. T., L. M. Ying, J. J. Green, S. Balasubramanian, and D. Klenerman. 2003. Ultrasensitive coincidence fluorescence detection of single DNA molecules. *Anal. Chem.* 75:1664–1670.

Li, J., D. Stein, C. McMullan, D. Branton, M. J. Aziz, and J. A. Golovchenko. 2001. Ion-beam sculpting at nanometre length scales. *Nature.* 412:166–169.

Meller, A., L. Nivon, and D. Branton. 2001. Voltage-driven DNA translocations through a nanopore. *Phys. Rev. Lett.* 86:3435–3438.

Morgan, H., M. P. Hughes, and N. G. Green. 1999. Separation of submicron bioparticles by dielectrophoresis. *Biophys. J.* 77:516–525.

Pohl, H. A. 1978. Dielectrophoresis. Cambridge University Press, Cambridge, UK.

Smith, S. B., and A. J. Bendich. 1990. Electrophoretic charge-density and persistence length of DNA as measured by fluorescence microscopy. *Biopolymers.* 29:1167–1173.

Stellwagen, N. C., C. Gelfi, and P. G. Righetti. 1997. The free solution mobility of DNA. *Biopolymers.* 42:687–703.

Vercoutere, W., S. Winters-Hilt, H. Olsen, D. Deamer, D. Haussler, and M. Akeson. 2001. Rapid discrimination among individual DNA hairpin molecules at single-nucleotide resolution using an ion channel. *Nat. Biotechnol.* 19:248–252.

Washizu, M., and O. Kurosawa. 1990. Electrostatic manipulation of DNA in microfabricated structures. *IEEE Trans. Ind. Appl.* 26:1165–1172.

Ying, L. M., A. Bruckbauer, A. M. Rothery, Y. E. Korchev, and D. Klenerman. 2002. Programmable delivery of DNA through a nanopipet. *Anal. Chem.* 74:1380–1385.